Inclusive Higgs boson and dijet production via Double Pomeron exchange

M. Boonekamp[*], R. Peschanski[†] and C. Royon[‡]

We evaluate Higgs boson and dijet cross-sections at the Tevatron collider via Double Pomeron exchange when accompanying particles in the central region are taken into account. Such *inclusive* processes, normalized to the observed dijet rate observed at run I, noticeably increase the predictions for tagged (anti)protons in the run II with respect to *exclusive* ones, with the potentiality of Higgs boson detection.

1. Not only recently, Higgs boson and dijet production via Double Pomeron (DP) exchange have attracted attention. It has been shown [1] that a non negligeable fraction of events with double colour singlet exchange features may appear. The calculation was based on a Pomeron model formulated as a pair of non-perturbative QCD gluons. However, the lack of solid QCD theoretical framework for diffraction makes a theoretical determination difficult. Predictions with many different mechanisms appeared [2] since then without clear consensus on the expected rate at hadron colliders. An evaluation of experimental possibilities [3] has given the prediction of a discovery potential for the Higgs boson through diffraction using outgoing (anti)proton tagging and a missing mass method. However, this evaluation again strongly depends on the theoretical framework.

In the present paper our aim is to give predictions based on *inclusive* Higgs boson and dijet production at the Tevatron collider via DP exchange. Indeed, so far, the predictions have been based on *exclusive* production without taking into account the accompanying particles in the central rapidity region. This accompanying radiation is unavoidable and is present in dijet production, a DP process already detected at the Tevatron [4]. This is obvious from the observed dijet over total mass fraction spectrum which is very different from the one expected in absence of radiation.

In fact, the evaluations contained in the present paper may have a triple phenomenological interest. **i)** Taking into account the accompanying particles allows one to normalize the theoretical predictions to the observed dijet rate and thus can be translated into a more constrained prediction for the Higgs boson. **ii)** The *inclusive* cross-sections are expected to be larger than the *exclusive* production mode **iii)** The signal/background ratio has to be evaluated differently in *inclusive* and *exclusive* events.

In the following we use the Bialas-Landshoff *exclusive* model for Higgs boson and heavy flavor jet production [1] as a starting point. We modify it in order to take into account *inclusive* Higgs boson and dijet production and the addition of light quark jets and gluon jets (not included in the analysis of Ref. [1]) . We show that we are able to reproduce up to a scale (which will be fixed from experiment) the observed distributions, in particular the dijet mass fraction spectrum. Using the same framework, we give predictions for *inclusive* Higgs boson production via DP exchange at the Tevatron.

The main lesson of our study is that, if the signal/background ratio can be maintained at a reasonable level when associated central radiation is allowed, an interesting discovery potential for the Higgs boson particle at the Tevatron run II can be expected in double (anti)proton tagged experiments. It is materialized in table I for the number of events as a function of M_H depending on experimental cuts and decay products.

Note that theses estimates are sizeably higher than the more recent *exclusive* production predictions [2]. The inclusion of all *inclusive* production modes of dijets allow us to fix the estimated proportion of quarks over gluon jets. It is small but not negligeable, contrary to the *exclusive* production. Thus DP production of dijets cannot be called a pure "gluon factory" (cf. last paper of Ref. [2]). One reason of this difference is for *exclusive* production the helicity conserving suppression of dijet production into quark jets vs. gluon jets which is absent in *inclusive* production. This re-normalization, in turn, enhances the prediction for Higgs boson production via the $\bar{t}t$ loop.

2. Let us introduce the formulae for Higgs boson and dijet production cross-sections via DP exchange. In the *exclusive* channel [1] one writes;

$$d\sigma_H^{excl} = C_H \left(\frac{s}{M_H^2}\right)^{2\epsilon} \delta\left((1-x_1)(1-x_2)-M^2/s\right) \prod_{i=1,2} \left\{\frac{dx_i}{x_i}\, d^2 v_i\, (1-x_i)^{\alpha' v_i^2}\, \exp\left(-2\lambda v_i^2\right)\right\} ,$$

[*]CEA, SPP, DAPNIA, CE-Saclay, F-91191 Gif-sur-Yvette Cedex, France
[†]*idem,* SPhT
[‡]*idem,* SPP and BNL, Upton, NY (USA), Texas U at Arlington (USA)

$$d\sigma_{\bar{Q}Q}^{excl} = C_{\bar{Q}Q} \left(\frac{s}{M_{\bar{Q}Q}^2}\right)^{2\epsilon} F_{\bar{Q}Q}(\rho)\, \delta^2 \left(\sum_{i=1,2}(v_i+k_i)\right) \prod_{i=1,2} \left\{\frac{dx_i}{x_i}\, d^2v_i\, d^2k_i\, (1-x_i)^{\alpha'v_i^2}\, \exp\left(-2\lambda v_i^2\right)\right\}, \qquad (1)$$

for a Higgs boson of mass M_H and two heavy quark jets (of total mass $M_{\bar{Q}Q}$), respectively. $\alpha(t) = 1 + \epsilon + \alpha't$ for the Pomeron trajectory ($\epsilon \sim .08, \alpha' \sim .25 GeV^{-2}$), $x_{1,2}$ ($> .9$) are the fraction of momentum of the outgoing p and $\bar{p}$, $v_{1,2}$, their 2-transverse momenta, $k_{1,2}$, those of the outgoing quark jets, $\lambda \sim 4 GeV^{-2}$ the slope of the Pomeron $p\bar{p}$ coupling, and the constants $C_H, C_{\bar{Q}Q}$ are normalizations containing various factors related to the hard matrix elements together with a common non-pertubative factor G^8 due to the non-pertubative gluon coupling [1]. Thus, the ratio $C_H/C_{\bar{Q}Q}$ is well defined while the overall normalization is not known, and will be determined by direct comparison with data.

For heavy quarks of mass m_Q and transverse mass $m_{T1,2}$ the hard contribution reads

$$F_{\bar{Q}Q}(\rho) = \frac{\rho\,(1-\rho)}{m_{T1}^2 m_{T2}^2}\,,\ \rho \equiv \frac{4m_Q^2}{M_{\bar{Q}Q}^2} \qquad (2)$$

which, up to colour factors included in the $C_{\bar{Q}Q}$, stands for the $gg \to \bar{Q}Q$ hard cross-section in the model. It is worthwhile to note that this cross section is proportional to m_Q^2, and thus is quasi zero for light quarks. This reflects the known zero helicity constraint of the quark jet production mechanism of Ref. [1] (For light quarks a zero appears in the forward anti(proton) direction, see dijet papers in [2]).

The method we propose to evaluate the inclusive production mechanisms for Higgs boson and dijets (including light quarks and gluons) is simple and not restricted to the Bialas-Landshoff model, even if we use it as a starting point. The main driving idea is that whatever the mechanism and normalization of the diffractive part of the process could be, the "hard" partonic interaction in the central region depends on the probability of finding the initial partons (quarks and gluons) in the central region at the short time. Since the overall partonic configuration is produced initially by the long-range, "soft" DP interaction, we will assume that, up to a normalization, the *inclusive* cross-section is the convolution of the "hard" *partons → Higgs boson, partons → jets* subprocesses by the probability of finding these partons in both Pomerons, see Fig.1. The working hypothesis is that the expected factorization breaking from soft color interaction will essentially affect the normalization through a renormalization of the Pomeron fluxes, which are not the same as in hard diffraction at HERA.

In this framework, QCD radiative corrections is the natural origin of *inclusive* production [9]. Indeed, our ansatz remarkably reproduces the dijet mass fraction seen in experiment which is obviously different from *exclusive* production, see Fig.2.

Hence, the Higgs boson and dijet *inclusive* cross-sections become:

$$d\sigma_H^{incl} = G_P(x_1^g,\mu)G_P(x_2^g,\mu)\,\frac{dx_1^g}{x_1^g}\,\frac{dx_2^g}{x_2^g}\,d\sigma_H^{excl}(s \to x_1^g x_2^g\, s),$$

$$d\sigma_{JJ}^{incl} = C_{\bar{Q}Q}\left(\frac{x_1^g x_2^g s}{M_{JJ}^2}\right)^{2\epsilon} F_{JJ}\, \delta^2\left(\sum_{i=1,2}(v_i+k_i)\right)\prod_{i=1,2}\left\{G_P(x_i^g,\mu)\,\frac{dx_i^g}{x_i^g}\,\frac{dx_i}{x_i}d^2v_id^2k_i\,(1-x_i)^{\alpha'v_i^2}\,\exp\left(-2\lambda v_i^2\right)\right\}, \quad (3)$$

where x_1^g, x_2^g define the fraction of the Pomerons' momentum carried by the gluons involved in the hard process, see Fig.1, and $G_P(x_{1,2}^g,\mu)$, are, up to a normalization, the gluon structure function in the Pomerons extracted from HERA experiments, see [7]. μ^2 is the hard scale (for simplicity kept fixed at $75 GeV^2$, the highest value studied at HERA). We neglected the processes initiated by quarks in the Pomeron which are negligeable in [7].

The dijet cross-section σ_{JJ} depends on two "hard" cross-sections $gg \to \bar{Q}^{(i)}Q^{(i)}$ and $gg \to gg$ [8]. This gives for 5 quark flavors ($i = 1 \cdot 5$)

$$F_{JJ} = \sum_i F_{\bar{Q}^{(i)}Q^{(i)}}\left(\rho^{(i)}\right) + 27\, F_{gg}\left(\rho^{gg}\right)\,;\ \rho^{(i)} \equiv \frac{4\,m_{T1}^{(i)}m_{T2}^{(i)}}{M_{\bar{Q}^{(i)}Q^{(i)}}^2};\ \rho^{gg} \equiv \frac{4\,p_{T1}p_{T2}}{M_{gg}^2}\,,$$

$$F_{\bar{Q}^{(i)}Q^{(i)}} \equiv \frac{\rho^{(i)}}{m_{T1}^{(i)}m_{T2}^{(i)}}\left(1-\frac{\rho^{(i)}}{2}\right)\left(1-\frac{9}{16}\,\rho^{(i)}\right)\,;\ F_{gg} \equiv \frac{1}{p_{T1}^2 p_{T2}^2}\left(1-\frac{\rho^{gg}}{4}\right)^3. \qquad (4)$$

27 stands for the colour factor fraction between gluon jets and quark jets partonic cross-sections [8]. Note that from now on , the $gg \to \bar{Q}^{(i)}Q^{(i)}$ cross section is proportional to *transverse* and not to rest quark masses. Thus, all 5 quark flavors sizeably contribute to the dijet cross-section. The quark contribution remains smaller, due to the color factor

and to the $\sim 1/p_T^4$ behaviour of the gluon exchange cross-section compared to the $\sim 1/(p_T^2 M_{Q^{(i)}Q^{(i)}}^2)$ one of the quark exchange cross-section but is no more suppressed by the helicity constraint.

3. The first step we perform is a comparison of our results with the measurements performed at Tevatron, in the CDF experiment [4]. To this end, we interfaced our generator with a fast simulation of the D0 and CDF detectors, namely SHW [10]. We chose as gluon content of the pomeron the result of the H1 "fit 1" performed in Ref. [7]. Note that the gluon density is used only up to the normalisation of the flux. We normalize our dijet cross section prediction with the CDF one.

We first compare our results for the dijet mass fraction with the measurement of the CDF collaboration [4] in DP events. A tagged antiproton with $0.035 \leq \xi_{\bar{p}} \leq 0.095$ and $|t| < 1$ GeV^2 was required where $\xi_{\bar{p},p} \equiv 1 - x_{1,2}$ is the momentum faction of the $\bar{p}, p$ carried by the corresponding pomeron. This quantity is reconstructed using the roman pot detectors installed by the CDF collaboration. After the CDF cuts to tag an antiproton and the fast simulation of the detector, we obtain a cross section of 14.4 nb, to be compared with the CDF measurement of 43.6 nb. At the present stage, at least two aspects are lacking in our study : firstly, our cross-section formulae do not include dissociation of the outgoing (anti)protons. Secondly, some (difficult to evaluate) fraction of the proton-tagged events seen in experiment are in fact fake tags, coming namely from excited N* states leaving an energetic decay proton in the detector. Both effects contribute to enhance the measured cross-section, and thus the difference between our prediction and the measured value [1]. We thus scale up our cross-sections by a factor $43.6/14.4 \sim 3$. As shown in Fig. 2, the dijet mass fraction spectrum is well reproduced. The CDF measurement could clearly not be described without radiation since the obtained dijet mass fraction would peak near one, up to detector resolution effects.

We can now give predictions for the Higgs boson production cross sections in double diffractive events, by scaling our results by the abovedetermined factor . The results are given in Table 1, first column. We note the high values of the cross-sections, which predict[2] more than 10 events per fb^{-1} for a Higgs boson mass below 140 GeV.

After interfacing the generator with the fast simulation package SHW [10], we can estimate the rates which could be observed in the experiments. The experimental resolution and acceptances of the roman pot detectors have been chosen to be similar to the D0 ones for dipole detectors, namely the t-resolution is $0.1\sqrt{t}$, t-acceptance $|t| \leq 0.5$ GeV^2, ξ-resolution 0.2 %, and the ξ-acceptance 100% if $\xi > 0.04$, 0% if $\xi < 0.01$ and linear between 0 and 100% if $0.01 < \xi < 0.04$ [11]. The tagging efficiency (see column 2 of Table 1) is quite good if one uses dipole detector on each side. To be able to trigger these events, some activity inside the central detector will be required, and we give in Table 1, third column, the number of events after requiring at least two jets of $p_T > 30$ GeV [3].

To enhance the signal to background ratio, it is possible to cut on the proton and antiproton tagged energy at 930 GeV (see Fig.3a), on the jet topologies (the jets coming from Higgs boson events are more central) and on the reconstructed mass distribution using the missing mass method [3] (see Fig.3b, and Fig.4). We slightly modified the original method to partly take into account radiation and define $M_H = \sqrt{\xi_p \xi_{\bar{p}} S} \frac{E_{jet1} + E_{jet2} + E_p + E_{\bar{p}}}{2E_{beam}}$ where the E_{jeti} are the leading two jets energies, E_p and $E_{\bar{p}}$ the tagged p and $\bar{p}$ energies. We notice that the missing mass method is not working so nicely when radiation is included. It is however still a competitive method to reduce background and reconstruct the Higgs boson mass[4]. The background over signal ratio will be detailed in Ref [5]. Since we obtain quite high cross-sections, other Higgs boson decay channels with smaller branching ratios, like $H \to \tau^+\tau^-$ (about 10% of Higgs boson decay, see table 1) or $H \to W^+W^-$ are of very high interest since the expected background is very small. This will be further discussed in Ref. [5].

---

[1]Note that the CDF cross section was measured after kinematical cuts on the proton side: $0.01 \leq \xi_p \leq 0.03$. This cut is difficult to reproduce using a fast simulation of the detector since it is very sensitive to the energy measurement inside the main CDF detector (the proton is not tagged). Thus, we did not apply this cut on our cross section. If one tries to apply these cuts in our fast simulation program, one obtains a cross-section two or three times smaller depending on the energy corrections. We chose not to apply these additional factors to be on the safe side concerning our predictions on the numbers of Higgs boson events. Thus, our Higgs boson event rates may be conservative by a factor 2 to 3 if one takes into account this effect.

[2]The expected luminosity is between 20 and 25 fb^{-1} per experiment for run II.

[3]This allows us to enhance our signal/background ratio (the $b\bar{b}$ diffractive background without any cuts is estimated to be about $2.3 \, 10^7$ events per fb^{-1}, and becomes about $8.3 \, 10^4$ events after those p_T cuts), as shown in Fig.3 c,d. When we compare Fig.2 c,d, we also note that radiation is more important for dijet events than for Higgs boson events, since the distribution for dijet events is more shifted to the left after radiation than the Higgs boson one. Hence, the p_T cut is more efficient after radiation.

[4]Due to radiation effects which escape mostly into the beam pipe, the missing mass method cannot work as it stands and is modified by radiation. However, it will be very useful to perform constrained fits and to have different ways of reconstructing the Higgs boson mass.

ACKNOWLEDGMENTS

REFERENCES

[1] J.D. Bjorken, *Phys.Rev.* **D47** (1993), A. Bialas and P.V. Landshoff, *Phys. lett.* **B256** (1990) 540, A. Bialas and W. Szeremeta, *Phys. lett.* **B296** (1992) 191, A. Bialas and R. janik, *Zeit. für. Phys.* **C62** (1994) 487.

[2] *Higgs boson:* J-R Cudell and O.F. Hernandez, *Nucl. Phys.* **B471** (1996) 471; E.M. Levin hep-ph/9912403 and referencies therein; V.A. Khoze, A.D. Martin and M.G. Ryskin, *Eur. Phys. J.* **C19** (2001) 477 and references therein.
Dijets: J. Pumplin, , *Phys. Rev.* **D52** (1995) 1477; A. Berera and J.C. Collins, *Nucl. Phys.* **B474** (1996) 183; A.D. Martin, M.G. Ryskin and V.A. Khoze, *Phys. Rev.* **D56** (1997) 5967; A. Berera, *Phys. Rev.* **D62** (2000) 015015;
Higgs boson and dijets: V.A. Khoze, A.D. Martin and M.G. Ryskin, hep-ph/0006005; V.A. Khoze, hep-ph/0105224 and references therein.

[3] M.G. Albrow and A. Rostovtsev, hep-ph/0009336.

[4] T. Affolder et al., CDF Coll. , *Phys. Rev. Lett.* **85** (2000) 4215.

[5] A detailed account of the model, the generator and the signal/background discussion will be available soon: M. Boonekamp, R. Peschanski and C. Royon, to appear.

[6] T. Affolder et al., CDF Coll. , *Phys. Rev. Lett.* **84** (2000) 5043.

[7] C. Royon, L. Schoeffel, J.Bartels, H.Jung, R.Peschanski, *Phys. Rev* **D63** (2001) 074004. The gluon structure function is obtained from the parametrization called H1 *fit1*.

[8] B.L. Combridge and C.J. Maxwell, *Nucl. Phys.* **B239** (1984) 429. Note a factor 2 difference with the coefficients used in the last paper of [2].

[9] We thank M. Peskin for this remark.

[10] *SHW, a fast simulation package for D0 and CDF detectors*, see www.physics.rutgers.edu/jconway/soft/shw/shw.html.

[11] *Proposal for a Forward Proton Detector at D0*, D0 Collab. (1997), Proposal P-900 to Fermilab PAC.

TABLE

$M_{Higgsboson}$	(1)	(2)	(3)	(4)	(5)
100	26.6	18.5	5.7	1.9	0.2
110	21.6	14.0	5.3	1.3	0.7
120	17.4	9.8	4.8	1.0	1.9
130	13.8	6.1	3.2	0.6	3.3
140	10.6	2.9	1.8	0.3	4.2
150	8.0	1.0	0.8	0.1	5.0
160	5.7	0.2	0.1	0.0	4.5
170	3.7	0.0	0.0	0.0	2.9

TABLE I. *Number of Higgs boson events for 1 fb^{-1}.* The first column gives the number of events at the generator level (all decay channels included), and the other columns after a fast simulation of the detector. The second colum gives the number of events decaying into $b\bar{b}$ tagged in the dipole roman pot detectors (see text), the third one requiring additionally at least two jets of $p_T > 30 GeV$, the fourth one gives the number of reconstructed and tagged events when the Higgs boson decays into τ, and the fifth one when the Higgs boson decays into W^+W^- (in this channel, the background is found to be negligible).

FIGURES

Figure 1

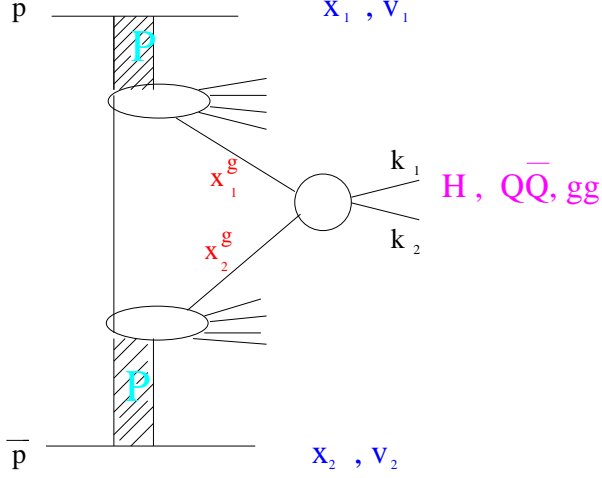*Inclusive production schemme.*

x_i, v_i are the longitudinal and transverse 2-momenta of the diffracted (anti)proton, x_i^g, the Pomeron fraction momentum brought by the gluons participating in the hard cross-section, k_i, the transverse 2-momenta of the outgoing jets in the central region from quarks, gluons or the $\bar{b}b$ decay products of the Higgs boson.
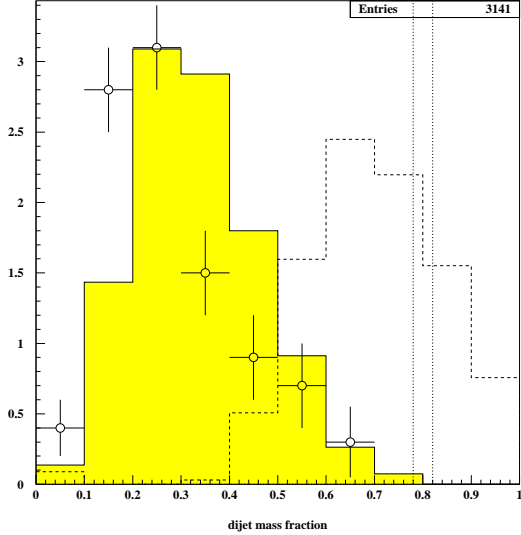

Figure 2

Comparison of the dijet mass fraction obtained in our model and CDF data (open circles).

With radiation: The shaded distribution is the dijet distribution after radiation and simulation of the detector.

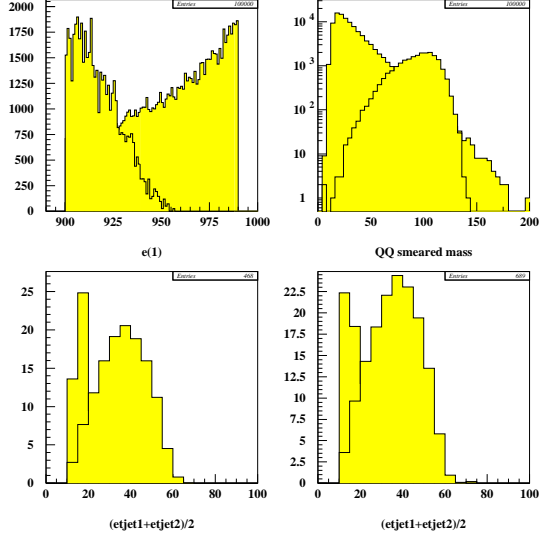*Without radiation:* Dotted line: distribution at generator level; Dashed line: after simulation of the detector.

Figure 3

Comparison of diffractive dijet and Higgs boson distributions.
the Higgs boson distributions are here always on the right of the $\bar{b}b$ distribution. Fig (3a, up left) gives the energy distribution of the tagged proton or antiproton, Fig (3b, up right) the leading dijet mass distribution, Fig (3c, down left) the mean leading two jet transverse energy in case radiation is added, and Fig (3d, down right) is the same plot without radiation. Normalisation is arbitrary in all figures.
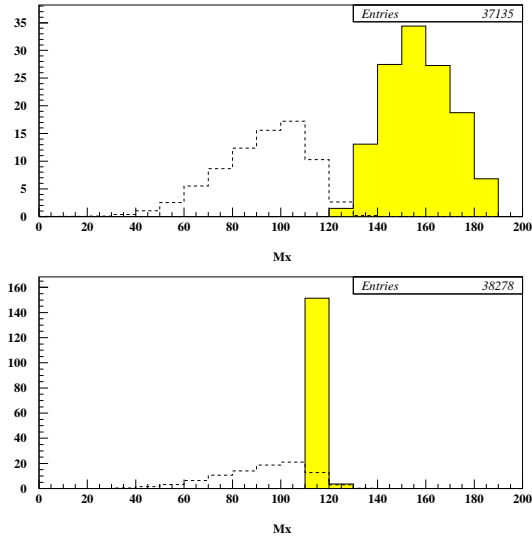

Figure 4

Higgs boson mass reconstruction. On top, with radiation, on bottom, without. The grey distribution is the result of the missing mass method, and the dashed line is the leading dijet mass distribution.

6